Elkholy, A., Hussein, M., Gomaa, W., Damen, D., & Saba, E. (2019). Efficient and Robust Skeleton-Based Quality Assessment and Abnormality Detection in Human Action Performance. *IEEE Journal of Biomedical and Health Informatics*. https://doi.org/10.1109/JBHI.2019.2904321

Efficient and Robust Skeleton-Based Quality Assessment and Abnormality Detection in Human Action Performance

Amr Elkholy, *Student Member, IEEE,* Mohamed E. Hussein, *Member, IEEE*, Walid Gomaa, Dima Damen, *Member, IEEE* and Emmanuel Saba

***Abstract*—Elderly people can be provided with safer and more independent living by the early detection of abnormalities in their performing of actions and the frequent assessment of the quality of their motion. Low-cost depth sensing is one of the emerging technologies that can be used for unobtrusive and inexpensive motion abnormality detection and quality assessment. In this study, we develop and evaluate vision-based methods to detect and assess neuromusculoskeletal disorders manifested in common daily activities using 3D skeletal data provided by the SDK of a depth camera (e.g., MS Kinect, Asus Xtion PRO). The proposed methods are based on extracting medically-justified features to compose a simple descriptor. Thereafter, a probabilistic normalcy model is trained on normal motion patterns. For abnormality detection, a test sequence is classified as either normal or abnormal based on its likelihood, which is calculated from the trained normalcy model. For motion quality assessment, a linear regression model is built using the proposed descriptor in order to quantitatively assess the motion quality. The proposed methods were evaluated on four common daily actions—sit-to-stand, stand-to-sit, flat-walk, and gait on stairs—from two datasets, a publicly released dataset and our dataset that was collected in a clinic from 32 patients suffering from different neuromusculoskeletal disorders and 11 healthy individuals. Experimental results demonstrate promising results, which is a step towards having convenient in-home automatic health care services.**

***Index Terms*—Motion Abnormality Detection, Motion Quality Assessment, Computer-Aided Diagnosis**

I. Introduction

AUTOMATIC abnormal action performance detection and motion quality assessment are gaining increasing importance in the research community as a way of providing the elderly with safer independent living. Elderly people, in particular, are susceptible to developing neuromusculoskeletal disorders through different medical conditions such as Parkinson's disease (PD), stroke, etc. Nevertheless, the phenomenon of living alone has become increasingly common among the elderly worldwide [1]–[4], which puts them at a higher risk of falling down or suffering an injury. Early detection of the aforementioned disorders can prevent such serious circumstances.

The currently used approaches for detecting abnormal action performance and assessing motion quality take place at medical facilities where the patient is required to perform several standardized tests (e.g., walk, turn, sit down, stand up) while a specialist assesses the motion quality using traditional tools (e.g., stopwatch, questionnaire). Therefore, the patient is required to visit the clinic periodically, which could be a potential burden for him/her.

Therefore, our research aims to develop an automatic system for in-home motion abnormality detection and quality assessment. This system will allow for the earliest possible detection of abnormality, which will lead to providing the elderly with a safer life and reducing the cost and burden of frequent clinic visits.

Several methods exist for motion abnormality detection and quality assessment using different sensors such as full body sensing (e.g., Motion Capture (MoCap)) and wearable sensors [5]–[8]. However, these methods are obtrusive as some wearable sensors may cause inconveniences. Moreover, multiple sensors may have to be used together in certain MoCap systems. In addition, such technologies are either extremely expensive and limited to lab environments (MoCap) [9] or require consistent and frequent maintenance, e.g., battery charging for wearable sensors.

Unlike the sensor-based approaches, vision-based approaches offer an unobtrusive method for motion abnormality detection and quality assessment. Low-cost depth sensors (e.g., MS Kinect, Asus Xtion PRO) can provide the 3D skeletal data of the person moving in front of the camera. This type of data can illustrate the person's pattern of motion, which is essential for detecting abnormal action performance and assessing the quality of motion. Despite that the 3D sensing devices cannot be used in outdoor applications, they can be used for developing unobtrusive techniques for detecting abnormal action performance and predicting the motion quality (e.g., what is the degree of the abnormality if any exists?) indoor, as they can be mounted at home/clinic without being directly attached

A. Elkholy and W. Gomaa are with the Department of Computer Science and Engineering, Egypt-Japan University of Science and Technology (E-JUST), Alexandria, Egypt. e-mail: amr.elkholy@ejust.edu.eg, walid.gomaa@ejust.edu.eg.

M. E. Hussein is currenly with the Information Sciences Institute, Arlington, VA, USA. e-mail: mehussein@isi.edu.

A. Elkholy is on leave from the Faculty of Engineering, Tanta University, Tanta, Egypt.

M. E. Hussein and W. Gomaa are also with the Faculty of Engineering, Alexandria University, Alexandria, Egypt.

D. Damen is with the Department of Computer Science, University of Bristol, Bristol, BS8 1UB, UK. e-mail: Dima.Damen@bristol.ac.uk.

E. Saba is with the Department of Physical Medicine, Rheumatology and Rehabilitation Department, Faculty of Medicine, Alexandria University, Alexandria, Egypt. e-mail: emmanuel.saba@alexmed.edu.eg

978-1-5386-5541-2/18/$31.00

to the patient's body and potentially inconveniencing them.

While there are numerous works for depth-based and skeleton-based activity recognition [10], our work focuses on abnormal action performance detection and assessment. A number of methods have been proposed for detecting abnormal events, such as falling, using depth cameras [11]–[15]. In contrast, our proposed method for abnormality detection aims at detecting the abnormal performance of normal daily activities.

On the other hand, another group of methods [16]–[19] focus on abnormal motion detection/classification for specific actions; hence, for these methods, action-specific features are extracted (e.g., stride time, stride/step length, walking speed, hip angles, hand joints). However, these features/parameters only suit specific actions (e.g., gait [16]–[18], sit-to-stand and reach assessment [19]) and generally cannot be applied to other daily activities. Another piece of work exists [20] for quantitatively evaluating neuromusculoskeletal disorders by measuring specific parameters such as step size, postural swing level, arm swing level, and stepping time. However, in addition to measuring action-specific parameters, this method is limited to periodic actions or repeated sequences of non-periodic actions. In another method, a sequence of joint positions (e.g., hand, elbow) is stored as a reference, and the similarity between the stored and the captured joint positions sequence is measured using Dynamic Time Warping (DTW) for the purpose of testing [21]. However, this method evaluates a specific joint's motion as compared to a reference motion for that joint, not the overall action performance; furthermore, this method is tailored for a particular set of prescribed exercises. In contrast, our method is general enough to cover multiple types of motions rather than focusing only on a specific motion class (e.g., walking) or motion type (e.g., periodic) and evaluates the entire action performance.

The work by Tao, et al. [22] is of particular relevance to ours. In this work, a method is proposed for motion quality assessment using skeletal data. The method depends on extracting common low-level features, such as joint positions, pairwise joint distances, pairwise joint angles, and joint velocities, and then reducing the dimensionality of the extracted feature vector using dimensionality reduction techniques, which require extra computational time and storage. Our methods also rely on skeletal data; however, they directly extract an extremely small number of features that possess very high representational power for classifying the action performance into normal or abnormal and predicting its quality score. Furthermore, the simplicity of the proposed method renders it appropriate for working in real-time, when required, and operating without processing backlogs, regardless of the level of activity in the scene, even on low processing-power platforms.

In this paper, we have enhanced, extended, further analyzed, and studied the effectiveness of a method we first introduced in [23] on a more realistic dataset. We have introduced a new dataset collected from patients with different types/degrees of neuromusculoskeletal disorders while performing three types of actions—walking, standing up, and sitting down. This new dataset is used in this paper to confirm the efficiency of our proposed features in detecting and assessing motion disorders in realistic scenarios.

We have proposed different normal motion models that rely on our simple action-independent descriptor, which encodes both the spatial and the temporal characteristics of the motion. The proposed descriptor consists of three medically justified and highly predictive features: asymmetry, velocity magnitude, and Center of Mass (CoM) trajectory deformation[1]. These features are computed from the 3D skeletal data extracted from the SDK of a depth sensor that can be mounted at home or a clinic.

For abnormality detection, we have built a probabilistic normalcy model using features extracted by our proposed descriptor from normal sequences only. The reason behind building an action normalcy model is that the abnormality in motion is diverse and cannot be specified by certain samples of abnormal action performance. While treating the problem as a classification problem might yield better results, it may not generalize well to abnormalities not seen in the dataset. Instead, we have built a normalcy model for each action using normal sequences and for testing a sequence, we have evaluated the fitness of the sequence to that model. In other words, our method measures the deviation of the action performance from the normal action performance model, and this deviation reflects the likelihood of the action performance being normal/abnormal.

In contrast, for motion quality assessment, we have built a linear regression model using the proposed descriptor. The function of this model is to predict an assessment score for the action performance, which reflects the degree of abnormality in performing the action. The model is trained on the ground truth scores provided by a professional physiatrist.

We have evaluated our proposed methods on two different datasets—a publicly released dataset [22] and our collected dataset, E-JUST Motion Quality Assessment (EJMQA). Both datasets include different actions (e.g., walking, sitting, standing) and different types of neuromusculoskeletal disorders (e.g., Parkinson's disease (PD), stroke, freezing). Results show that our proposed descriptor can capture abnormal action performance for different actions with high accuracy and can be effectively used for assessing the quality of action performance, even in real-life applications.

II. METHODS

The block diagram of the proposed methods is illustrated in Fig. 1. The first method is responsible for detecting abnormal action performance, which was first presented [23] and enhanced in this paper while the second method is responsible for quantitatively assessing the quality of action performance. The methods begin by performing a data preprocessing for the skeletal data, followed by descriptor construction. Then, a probabilistic/regression model is trained and, finally, the test sequences are evaluated. These steps are discussed in detail in the following subsections.

[1]Center of Mass (CoM) trajectory deformation feature is a replacement for the Base of Support (BOS) feature presented in our initial work [23].

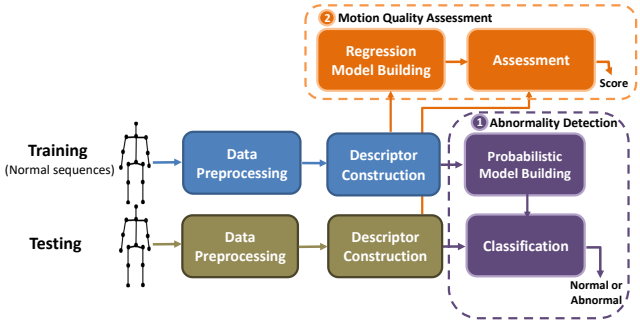

Fig. 1: Block diagram of the proposed methods for motion abnormality detection and assessment

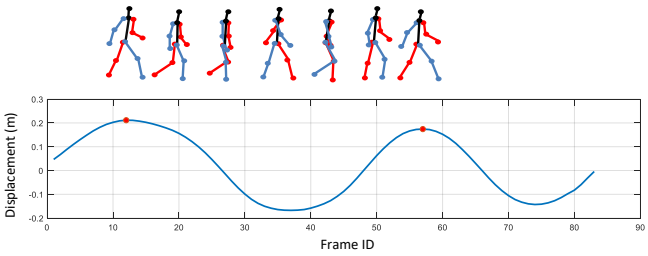

Fig. 2: Feet displacement during gait

A. Data Preprocessing

A data preprocessing step is first applied to the noisy skeletal data (joints positions) that is provided by the depth camera SDK. This step includes noise removal, action instance cropping, and coordinate scaling. The noisy skeletal data sequence is first cleaned using a uniformly weighted averaging filter of length 5. Then, the frames of the action instance are cropped from the sequence. For the walking action, we extract one gait cycle using the horizontal displacement between the feet joints in the motion direction, i.e., the Z-axis if the motion is perpendicular to the camera plane (frontal-view) or the X-axis if the motion is parallel to the camera plane (side-view). The gait cycle begins at the heel-strike of one foot (represented by the maximum displacement between feet joints) and ends with the heel-strike of the same foot for the next cycle as illustrated in Fig. 2. For the sitting down and standing up actions, cropping is done using a velocity magnitude threshold that excludes non-motion frames at the beginning and the end of the sequence. For the gait on stairs action, we used the same method as the walking action. Finally, the 3D joint coordinates are scaled so that each of the three dimensions lies in and covers the interval $[0, 1]$ over the entire sequence. This is to render the features invariant to skeleton size (i.e., scale) and location (i.e., translation) with respect to the camera.

B. Descriptor Construction

After data preprocessing, our proposed descriptor is constructed by extracting a low number of medically-inspired features that capture abnormality in action performance. These features are asymmetry, velocity magnitude, and center of mass (CoM) trajectory deformation. They are all computed from the 3D skeletal data. The asymmetry feature measures the asymmetric motion of the left and right body parts during action performance while the velocity magnitude feature measures the speed of performing an action. Finally, the center of mass (CoM) trajectory deformation feature measures the dissimilarity between the vertical displacement trajectory of the CoM during the action performance and the normal pattern of such a trajectory.

The significance of these features for motion quality assessment can be observed by inspecting how they look in normal sequences vs. how they look in abnormal ones. To illustrate the significance of the asymmetry and velocity magnitude features, we have created a Motion History Image (MHI) [24], [25] in order to demonstrate the difference between the normal and abnormal performance of different actions. MHIs are used to represent the motion in a video sequence as a single image where darker pixels correspond to earlier motion, and brighter pixels represent recent motion. Fig. 3 illustrates the MHI of sample sequences with normal and abnormal action performance for different actions. The asymmetry feature is clear in the abnormal action performance of the different actions Fig. 3 (a), (b), (c) as the left and right body part's movements are not symmetric along the action sequence; whereas the velocity magnitude feature can be observed in gait freezing Fig. 3 (d) in a darker color as the patient takes a longer time than healthy individuals to perform the action. For the center of mass (CoM) trajectory deformation feature, Fig. 4 illustrates the vertical displacement of the CoM of normal and abnormal subjects performing (a) one gait cycle, (b) the sitting down action, (c) the standing up action, (d) stairs action. We can observe from Fig. 4 that each action has a unique normal pattern (blue), and the existence of an abnormality deforms this pattern (red). The deformation can appear as cavities or bumps in the CoM vertical displacement trajectory, which makes the trajectory non-smooth like the normal one.

1) Asymmetry Feature: This feature can capture the asymmetric motion between the left and right body parts over the sequence of an action, which is a common trait for most neuromusculoskeletal disorders [26], [27]. On the other hand, the normal performance of common daily activities (e.g., walking, sitting down, standing up) reflects symmetric behavior between the left and right body parts over the sequence of an action.

Below is our algorithm for computing a value that reflects the degree of the motion asymmetry between the left and right body parts over the skeletal data sequence.

We start by splitting the body joints vertically into two overlapping groups as shown in Fig. 5. Then, for every pair of joints in each group, we compute the average distance over the sequence. Let D^L and D^R be the average pairwise distance matrices for the left and right body parts, respectively. The asymmetry feature can be represented by the Euclidean distance between the vectorized upper triangles of the two matrices, D^L and D^R. Letting A be the asymmetry feature, its computation can mathematically be expressed as

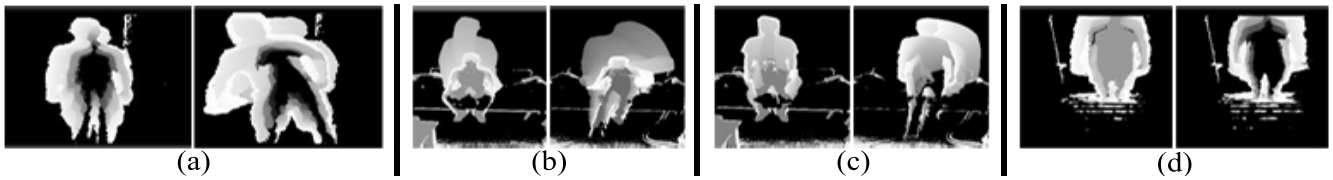

(a) (b) (c) (d)

Fig. 3: Motion History Image (MHI) for the four actions including normal (left image) and abnormal (right image) samples (a) Walking on flat surface (b) Sitting down (c) Standing up (d) Stairs

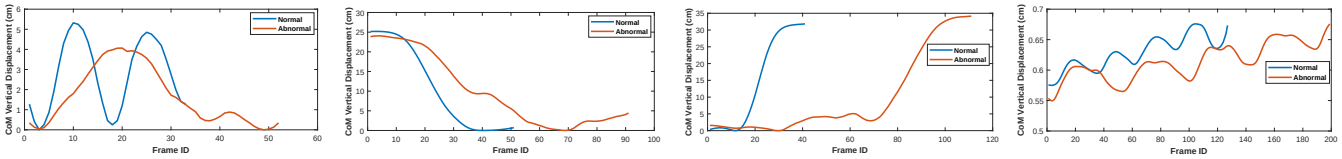

(a) (b) (c) (d)

Fig. 4: CoM vertical displacement trajectory for normal (Blue) and abnormal (red) action performance for a) One gait cycle (b) Sitting down (c) Standing up (d) Stairs actions (Figure best viewed in color)

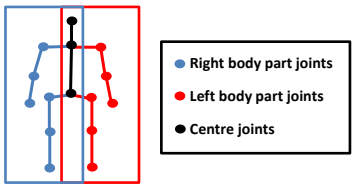

Fig. 5: The splitting of body joints for computing the asymmetry feature

$$D_{ij}^{P} = \frac{\sum_{t=1}^{n} \sqrt{(x_{it}-x_{jt})^2+(y_{it}-y_{jt})^2+(z_{it}-z_{jt})^2}}{n}, \quad \forall i,j \in N_P, P \in \{L,R\}, \tag{1}$$

$$A = ||\mathbf{uvec}(D^L) - \mathbf{uvec}(D^R)||, \tag{2}$$

where D^P is the left/right body part's average pairwise distance matrix, x_{it}, y_{it}, z_{it} are the 3D coordinates of the joint i at frame t, n is the number of frames in the action sequence, N_P is the set of joints in the left/right body part, and the **uvec**() operator outputs the vectorized upper triangle of its operand matrix.

The value of this feature represents an indicator for the degree of asymmetry between the movements of the two body parts over the sequence. Therefore, this value should be low for normal action performances and will become higher depending on the degree of abnormality when performing an action.

2) Velocity Magnitude Feature: This feature is responsible for detecting slow action performance as most neuromusculoskeletal patients perform their daily activities significantly slower [28], [29].

The velocity magnitude feature is extracted by computing the displacement magnitude for each body joint between two successive frames and calculating the average displacement magnitude over all joints between the two successive frames. We consider this average inter-frame joint displacement magnitude as an estimate for the average joint velocity magnitude. Therefore, for the whole sequence, we will have $n-1$ average velocities. Thereafter, we calculate the average a second time over frames. This will produce the average velocity magnitude during the motion over the entire sequence, which is expected to be low in the case of freezing or abnormally slow motion. In mathematical terms, the velocity magnitude feature V is computed as

$$V = \frac{\sum_{t=1}^{n-1} \sum_{i=1}^{N} \sqrt{(x_{i(t+1)}-x_{it})^2+(y_{i(t+1)}-y_{it})^2+(z_{i(t+1)}-z_{it})^2}}{(n-1)N}, \tag{3}$$

where N is the number of joints, and n is the number of frames.

3) Center of Mass (CoM) Trajectory Deformation Feature: Center of Mass (CoM) is defined as a single point where the mass of the body is concentrated. The CoM displacement during gait has been used to evaluate gait efficiency and specifically, the vertical displacement of the CoM during locomotion [30], [31]. The CoM vertical displacement trajectory has a unique pattern for normal action performance; however, motion disorders may deform this pattern as illustrated in Fig. 4. This deformation can appear in the form of cavities, bumps, or any other deviation from the normal smooth pattern. Hence, by measuring the amount of existing deformation in the CoM vertical displacement trajectory as compared to a normal reference trajectory, we can obtain insight into how normal/abnormal the motion is. Therefore, this feature is called the CoM trajectory deformation. We use this feature as the third feature of our general descriptor. The function of this feature is to first compute the vertical displacement of the CoM of the moving subject before measuring the dissimilarity between the computed trajectory and a normal representative reference trajectory selected from the training dataset [2]. To

[2]In order to select a representative reference, we have used the medoid of the training samples as a reference. The medoid is the sample whose average dissimilarity to all other samples in the dataset is minimal.

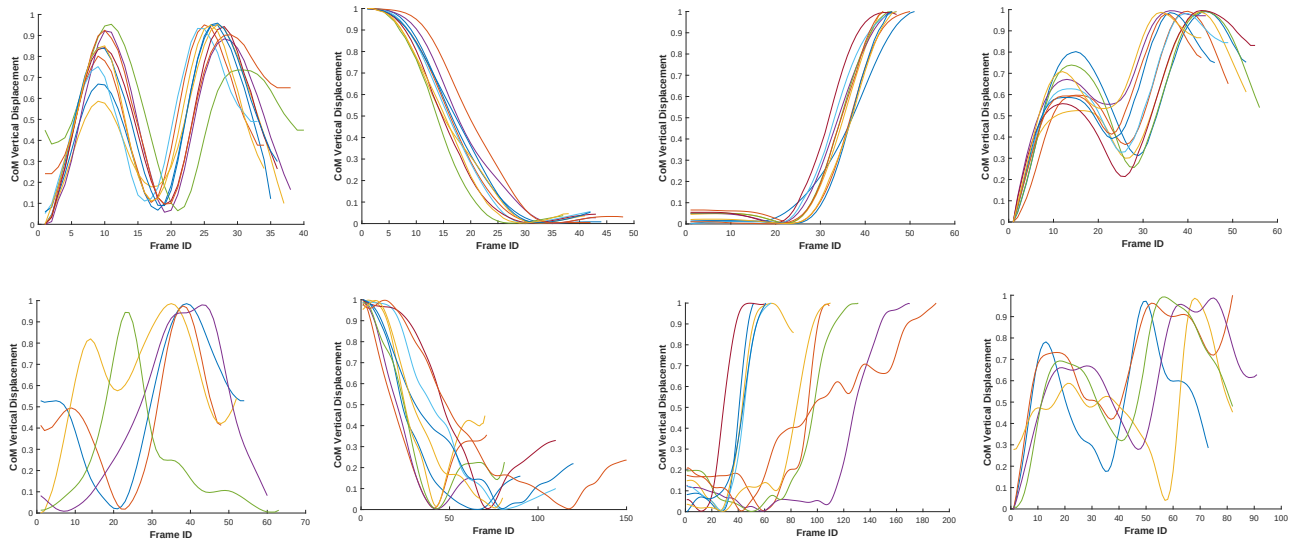

(a) One gait cycle (b) Sitting down (c) Standing up (d) Stairs

Fig. 6: CoM vertical displacement trajectories for normalized and aligned normal (Upper) and abnormal (Lower) samples for four different actions, where (a), (b) and (c) are taken from EJMQA dataset, and (d) is taken from SPHERE dataset (Figure best viewed in color)

compute the CoM of the moving subject, we apply the segmental method on the 3D joints data, from which the body mass segments fractions and the location of the mass centers were obtained [32]. Then, we used the following equations to compute the coordinates of the CoM of each segment:

$$x_{cm}(i) = X_P + (X_D - X_P).(\%CoM), \tag{4}$$

$$y_{cm}(i) = Y_P + (Y_D - Y_P).(\%CoM), \tag{5}$$

$$z_{cm}(i) = Z_P + (Z_D - Z_P).(\%CoM), \tag{6}$$

where $(x_{cm}(i), y_{cm}(i), z_{cm}(i))$ are the 3D coordinates of the center of mass of segment i, X_P, Y_P, Z_P are the 3D coordinates of the proximal end of the segment, X_D, Y_D, Z_D are the coordinates of the distal end of the segment, and %CoM is the CoM location from the proximal end to the disposal end. Finally, we use the following equations to compute the whole body CoM in each frame:

$$X_{cm} = \frac{\sum_i^n m_i.x_{cm}(i)}{M}, \tag{7}$$

$$Y_{cm} = \frac{\sum_i^n m_i.y_{cm}(i)}{M}, \tag{8}$$

$$Z_{cm} = \frac{\sum_i^n m_i.z_{cm}(i)}{M}, \tag{9}$$

where X_{cm}, Y_{cm}, Z_{cm} are the 3D coordinates of the whole body CoM, m_i is the mass of segment i, and M is the total body mass ($\sum_{i=1}^n m_i$).

Since we are interested in the vertical displacement, we compute the y-direction values, Y_{cm}, only. After computing the whole body CoM vertical displacement trajectory, the trajectory is normalized to the scale [0, 1]. Fig. 6 illustrates the normalized and aligned trajectories of different normal and abnormal samples, in which we can observe the normal pattern of each action and the deformed abnormal samples. Furthermore, the dissimilarity between the computed and reference trajectories is measured using Dynamic Time Warping (DTW). Dynamic time warping (DTW) is a non-linear sequence alignment algorithm that can measure the dissimilarity between two time-series signals with different lengths by determining the time alignment that maximizes the similarity (minimizes the distance) between the two signals.

This feature should return a value proportional to the degree of the deformation that exists in the vertical displacement trajectory of the CoM of the moving subject compared to the normal reference trajectory. This value should be low in case of normal action performance and become higher depending on the degree of abnormality.

C. Action Abnormality Detection

In this part, we propose a method using the proposed descriptor to detect the abnormality in motion. The method depends on building a probabilistic model with the extracted features from normal sequences (normalcy model) in training. For testing, we compute the likelihood for the test sequence, and based on a learned threshold, the system can decide whether the sequence is normal or not. Before building the model, we first normalize each feature in the training and testing data using Z-Score normalization.

Let $S_x(i)$ be the score of feature $x \in \{$Asymmetry, Velocity Magnitude, or CoM Trajectory Deformation$\}$. Then, the normalized score is given by

$$\overline{\mathrm{S}}_x(i) = \frac{S_x(i) - \mu_x}{\sigma_x}, \tag{10}$$

where μ_x and σ_x are the mean and the standard deviation of feature x, respectively and computed from the training data. The sample statistics are estimated using a robust estimate technique to cope with noise and outliers (we used Huber's

M-method [33] in our implementation).

1) Gaussian Mixture Model (GMM): We first tested our descriptor on a parametric generative probabilistic model, which is GMM. In this subsection, we first introduce the model, followed by a brief introduction of the Dirichlet Process Mixture Model (DPMM), which has been used to compute the number of GMM components.

We have built the model using features computed only from normal sequences to generate a normalcy model with the standard formulation of the GMM as

$$p(X|\lambda) = \sum_{i=1}^{M} w_i g(\boldsymbol{x}|\mu_i, \Sigma_i)\,, \tag{11}$$

where $\boldsymbol{x}$ is the 3D value in the three features space, $\lambda = \{w_i, \mu_i, , \Sigma_i\}$, w_i is the mixture weight, and M is the number of mixture components such that each component is a 3D Gaussian function expressed as

$$g(\boldsymbol{x}|\mu_i, \Sigma_i) = \frac{1}{(2\pi^{3/2})|\Sigma_i|^{1/2}} e^{\frac{-1}{2}(\boldsymbol{x}-\mu_i)' \Sigma_i^{-1}(\boldsymbol{x}-\mu_i)}\,, \tag{12}$$

where μ_i is the mean vector, and Σ_i is the covariance matrix. The mixture parameters were computed using Expectation Maximization (EM) [34].

An important issue in finite mixture modeling is the selection of the optimal number of components that represent the data. To address this issue, we have used the Dirichlet Process Mixture Model (DPMM) [35], which is a Bayesian non-parametric clustering approach that can infer the number of clusters. We started by learning the DPMM using the normal learning sequences by utlizing the Gaussian-Wishart distribution as the base distribution and the concentration parameter's default value, $\alpha = 1$. The DPMM components are learned using the Chinese Restaurant Process (CRP) and Gibbs sampling. Then, the number of mixture components learned from the training data is used as the number of components for the GMM.

For testing, we compute the likelihood of a testing sequence by evaluating the trained GMM and, hence, the likelihood can be used as a normalcy similarity measure. Further, with a learned threshold, the method decides if the sequence is normal or abnormal.

2) Kernel Density Estimation (KDE): The second model that has been used to test our descriptor is KDE as a non-parametric model with the standard KDE equations as

$$f_h(x) = \frac{1}{nh} \sum_{i=1}^{n} G(\frac{x - x_i}{h}), \tag{13}$$

where G is a Gaussian kernel function, x is the 3D training sample, h is the bandwidth that was computed using Silverman's method [36], and n is the number of training samples.

For testing, we also compute the likelihood of a testing sequence by evaluating the trained KDE and, with the selected threshold, the method decides if the sequence is normal or abnormal.

3) Threshold Selection: For both models, the threshold choice depends on the specific application requirements (i.e., maximum tolerable false alarm rate, equal error rate). Although the method works by fixing a threshold (according to specific application requirements), the evaluation in this paper uses metrics that do not depend on the threshold setting.

D. Motion Quality Assessment

To evaluate the quality of performing an action, we propose a regression-based method for predicting an assessment score, which can reflect the degree of abnormality in performing an action by providing a customized overall action performance score on the scale of (1–5), where 1 is the highest abnormality, and 5 is no-abnormality, i.e., normalcy.

In particular, for this task, we trained a multiple linear regression with interactions model, where the explanatory variables are the proposed features, and the dependent variable is the score as illustrated by Eq. (14).

$$Y = \beta_0 + \beta_1 x_1 + \beta_2 x_2 + \beta_3 x_3 + \beta_{12} x_1 x_2 + \beta_{13} x_1 x_3 + \beta_{23} x_2 x_3, \tag{14}$$

where Y is the predicted score, x_i is the feature value, β_i is the regression coefficients, and β_0 is the intercept.

To train and test the model, we have collected a dataset consisting of patients who have different degrees of motion disorders and have been evaluated by a professional specialist using a customized score that reflects the degree of abnormality. The details of the collected dataset and the evaluation criteria are illustrated in the next section.

Although the assessment scores in our dataset happened to be integer valued, the dependent variable in this task (i.e., the assessment score) is a real numeric variable and not a categorical one. Therefore, we have used ordinary regression rather than ordinal logistic regression (i.e., proportional odds model [37]).

We tested different ordinary regression models (i.e., linear regression, quadratic regression, linear Support Vector Regression (SVR), Gaussian SVR, and squared exponential Gaussian Process Regression (GPR)) and found that the best-fitting model for our data is the multiple linear regression model with interactions. A comparison of these models is provided in the results section.

III. Evaluation And Results

A. Datasets

To evaluate the proficiency of our proposed methods, we tested our methods on two different datasets while including different actions and neuromusculoskeletal disorders.

1) SPHERE dataset [22]: We first tested our method on a public dataset released by the University of Bristol [22]. The dataset contains four different common daily actions—gait on stairs, walking on a flat surface, sitting down, and standing up—each partitioned into training and testing sequences. The dataset was collected from healthy people feigning different types of abnormalities. This dataset was collected using two

different types of depth cameras (MS Kinect V2 and Asus Xtion PRO), in which the joint counts are different, i.e., MS Kinect V2 extracts 25 joints while Asus Xtion PRO extracts 15 joints [3]. For more details about the counts of training/testing samples, the reader is referred to our previous paper [23].

2) EJMQA dataset: To test the proposed methods on a more realistic dataset, we collected a new dataset from patients and healthy individuals performing the Timed Up and Go test (TUG). Our dataset includes the following actions: standing up, walking, and sitting down. This dataset was collected using the MS Kinect V2 with a frame rate of 30 fps and 25-joint skeletal data.

A customized evaluation sheet was conducted by a professional physiatrist to evaluate the patients with concentrating on the following traits: the degree of the asymmetry of motion and the speed of performing the action calculated using the time taken to complete the action. Then, an overall action performance score on the scale (1–5) was provided, in which a score of (1) represents high abnormality, and (5) represents normal action performance. Hence, the EJMQA dataset was divided into two categories based on the degree of abnormality; scores (1–2) represent a high abnormality while scores (3–4) represent a medium-to-low abnormality. The customization of the evaluation sheet is undertaken to measure the efficiency of the proposed features and the extent to which they match the professional physiatrist's evaluation. In addition to these features, the following data was collected: age, gender, height, weight, and gait type.

The dataset included 32 patients with abnormal gait, who were consecutively recruited from those attending the Outpatient Clinic of Physical Medicine, Rheumatology and Rehabilitation Department, Main University Hospital, Alexandria Faculty of Medicine. In addition to the patients, the study included 11 apparently healthy volunteers as a control group. The volunteers included medical staff, their relatives, patients relatives as well as students and faculty members from the Computer Science and Engineering Department at E-JUST. After a detailed medical history was taken, a careful clinical examination of all the patients was conducted with a concentration on musculoskeletal and neurological examination. The diagnosis of the medical condition was performed according to the standard diagnostic criteria.

The patients' mean age was 52.25 (SD: 16.60) years, with a range of 18–85 years. There were 13 female patients (40.6%). The control subjects' mean age was 37.18 (SD: 11.29) years, with a range of 27–64 years. There were eight males in the apparently healthy control group (72.7%). For the patients' group, the inclusion criterion was the presence of an abnormal gait while the exclusion criterion was the presence of acute infection or acute trauma. The study was explained to the participants, and an informed consent was submitted by each. The study had been approved by the ethics committee of the Faculty of Medicine, Alexandria University, Egypt.

[3]We used the 15 common joints between the two cameras; hence, we excluded the following joints from the data collected by MS Kinect V2: hand tip, hand thumb, wrist, ankle, spine shoulder, and spine mid.

This dataset was made publicly available upon request to help researchers in testing their proposed methods on a realistic dataset.

B. Abnormality Detection

Figures 7, 8, and 9 illustrate the distribution of the sequences of the SPHERE, EJMQA-High abnormality, and EJMQA-Med-Low abnormality datasets, respectively, in the 3D feature space; blue points represent normal training sequences, green triangles represent normal testing sequences, and red $\times$'s represent abnormal testing sequences.

To evaluate our method for motion abnormality detection, we used the following metrics: Area Under the Curve (AUC) of the Receiver Operating Characteristics (ROC) curve of sequence classification, Equal Error Rate (EER), Detection Rate (DR) at 1% False Acceptance Rate (FAR), and Detection Rate (DR) at 5% False Acceptance Rate (FAR).

We evaluated the proposed method of motion abnormality detection for each action of the two datasets, SPHERE and EJMQA. For the SPHERE dataset, it has already been divided by the authors into training and testing; therefore, we used the same division. For the EJMQA dataset, Table I illustrates the counts of normal and abnormal sequences/subjects for each action [4]. The normal sequences were divided into three groups of approximately equal sizes. Then, we tested our method three times, each time using two groups of the normal sequences for training and the remaining group for testing while all the abnormal samples were used for testing. Finally, we reported the mean results over the three times.

	Walking	**Sitting down**	**Standing up**
Normal	40 / 10	40 / 10	40 / 10
High Abnormal	21 / 9	19 / 8	19 / 8
Med-Low Abnormal	49 / 19	22 / 10	22 / 10

TABLE I: EJMQA Dataset Details (Sequences/Subjects)

For the SPHERE dataset, Fig. 7 illustrates the distribution of the samples of the different actions in the 3D feature space, and Table II illustrates the results achieved by applying our proposed feature descriptor to both models, i.e., GMM and KDE. The results are approximately the same as presented in [23]; however, we modified the following: first, the BOS feature represented in [23] was replaced by a more general feature, the CoM vertical displacement trajectory deformation. Despite achieving approximately the same results, the new feature can reveal more information about motion disorders diagnosis, especially in terms of actions other than walking. Second, for the walking and stairs actions, we applied our features descriptor after extracting one gait cycle using the method mentioned in the preprocessing subsection rather than applying the descriptor to the entire sequence. Third, the number of components for the GMM was selected automatically using DPMM.

We can observe from Fig. 7 that the proposed 3D feature space can separate the normal and abnormal action

[4]The counts of abnormal sequences/subjects differ from one action to another as the patient may perform one action abnormally while performing another in a normal manner.

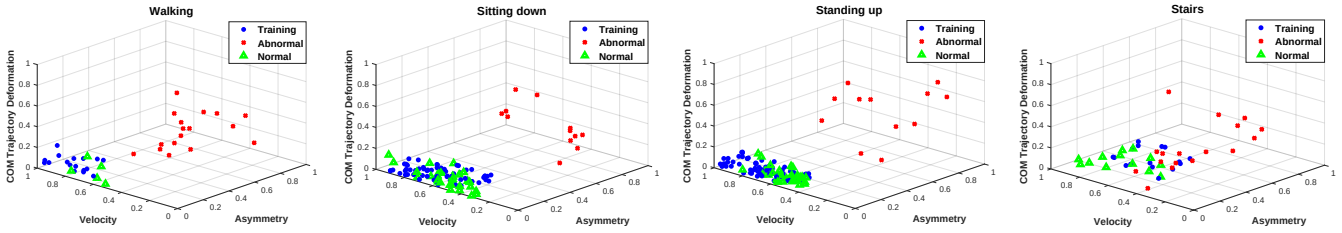

(a) (b) (c) (d)

Fig. 7: Distribution of the **SPHERE [22]** dataset's training and testing samples in the 3D feature Space (a) Walking (b) Sitting down (c) Standing up (d) Stairs (Figure best viewed in color)

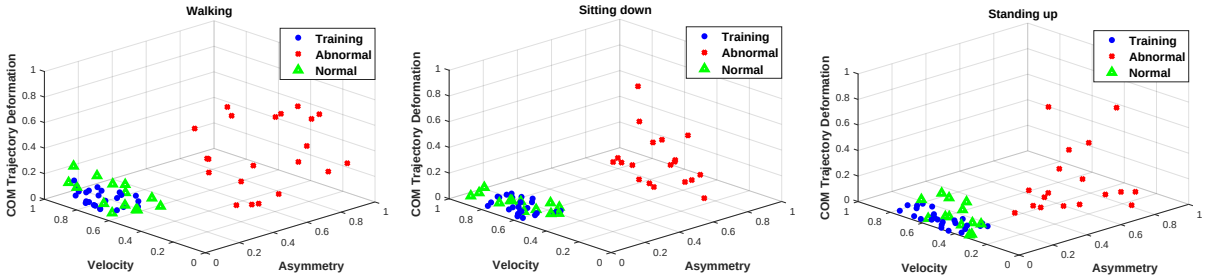

(a) (b) (c)

Fig. 8: Distribution of the **EJMQA-High abnormality** dataset's training and testing samples in the 3D feature space (a) Walking (b) Sitting down (c) Standing up (Figure best viewed in color)

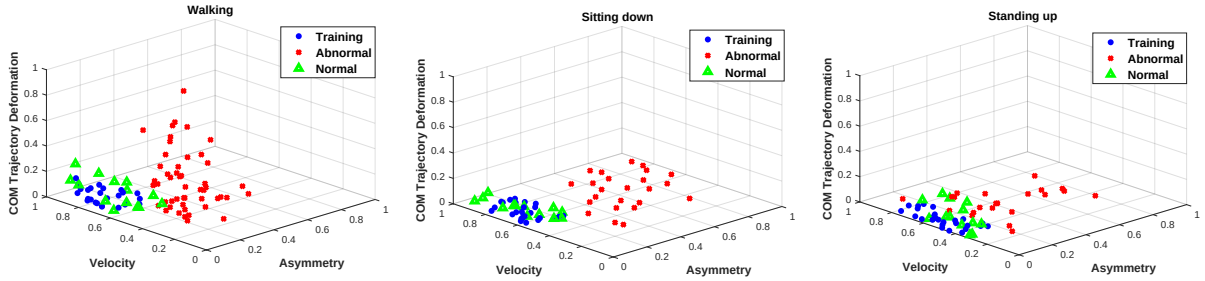

(a) (b) (c)

Fig. 9: Distribution of the **EJMQA-Med-Low abnormality** dataset's training and testing samples in the 3D feature space (a) Walking (b) Sitting down (c) Standing up (Figure best viewed in color)

performance samples, especially for walking, sitting down, and standing up actions with little confusion and overlap regarding the 'gait on stairs' action. We have explained this by the high dynamics of the gait on the stairs action and the high probability of occlusion in it, which decreases the accuracy of the estimated joint positions. Table II illustrates the classification accuracy, represented by AUC, EER, and DR. Our method was able to achieve AUC of 1 for walking, sitting down, and standing up using both models, while for the gait on stairs action, we achieved AUC of 1 using GMM and 0.98 using KDE.

Model	Metric	Walking	Sitting	Standing	Stairs
GMM	AUC	1	1	1	1
	EER	0	0	0	0
	DR at 1% FAR	1	1	1	1
	DR at 5% FAR	1	1	1	1
KDE	AUC	1	1	1	0.98
	EER	0	0	0	0.059
	DR at 1% FAR	1	1	1	0.85
	DR at 5% FAR	1	1	1	0.85

TABLE II: Abnormality Detection Results on SPHERE Dataset

For the EJMQA dataset, the abnormal part of the dataset is divided into two levels—high abnormality and med-low abnormality. The distributions of the dataset's walking, sitting down, and standing up samples in the 3D feature space for the two abnormality levels are illustrated in Fig. 8 and 9, respec-

Model	Metric	Walking		Sitting		Standing	
		High	Med-Low	High	Med-Low	High	Med-Low
GMM	AUC	1 ± 0	0.99 ± 0.008	1 ± 0	0.99 ± 0.002	1 ± 0	0.91 ± 0.047
	EER	0 ± 0	0.034 ± 0.043	0 ± 0	0.014 ± 0.024	0 ± 0	0.152 ± 0.069
	DR at 1% FAR	1 ± 0	0.88 ± 0.108	1 ± 0	0.97 ± 0.044	1 ± 0	0.46 ± 0.067
	DR at 5% FAR	1 ± 0	0.98 ± 0.041	1 ± 0	1 ± 0	1 ± 0	0.61 ± 0.091
KDE	AUC	1 ± 0	0.97 ± 0.03	1 ± 0	0.99 ± 0.05	1 ± 0	0.92 ± 0.05
	EER	0 ± 0	0.095 ± 0.05	0 ± 0	0.03 ± 0.05	0 ± 0	0.18 ± 0.09
	DR at 1% FAR	1 ± 0	0.75 ± 0.09	1 ± 0	0.95 ± 0.09	1 ± 0	0.57 ± 0.16
	DR at 5% FAR	1 ± 0	0.86 ± 0.14	1 ± 0	0.95 ± 0.09	1 ± 0	0.67 ± 0.15

TABLE III: Abnormality Detection Results on EJMQA Dataset using GMM and KDE (Mean ± Std)

tively. We can observe from the two datasets that the abnormal testing samples (red ×'s) become closer to the normal samples as the degree of abnormality gets lower and, hence, the discrimination accuracy becomes lower as illustrated in Table III using either GMM or KDE models. For the high abnormality dataset, the proposed method achieved zero misclassification rates (AUC equals 1 and EER of 0) while using both models for the three actions. This is due to the clear separation between normal and abnormal samples in the 3D feature space of the three actions as can be observed in Fig.8. Conversely, for the med-low abnormality dataset, we achieved less accuracy for the three actions as illustrated by Table III. The reason is that the EJMQA med-low abnormality dataset contains some subjects who mostly appear normal; however, they suffer from mild or weak abnormalities in motion. Therefore, the feature values associated with their actions significantly overlapped with those of the normal samples as can be observed in Fig. 9. This situation was not encountered in the SPHERE dataset, wherein the abnormalities were imitated by normal people. As a result, the abnormal action performances could have been exaggerated in the SHPERE dataset, which resulted in the clear feature space separation and, hence, in the better accuracy of our methods.

C. Motion Quality Assessment

Since the features' values are proportional to the degree of abnormality, we believe that these features can be used for the motion quality assessment task. Fig. 10 illustrates the average features' values across the different scores of abnormality of the EJMQA dataset. We can observe that our features' mean values are generally proportional to the degree of abnormality in the three actions.

In this subsection, we examine the regression-based model for estimating a motion quality score that reflects the existing degree of abnormality in performing an action. This function was examined only on the EJMQA dataset. This is due to the availability of the motion quality scores assisted by a professional physiatrist.

We tested different regression models, and each model was trained using the proposed features' values and the corresponding scores provided by the professional physiatrist. For testing, we used the proposed features' values, and the model estimated the quality score. Two-thirds of the sequences were used for training the regression model while the remaining one-third were kept for testing; the subjects in the training and testing sets are disjoint and selected at random. We performed

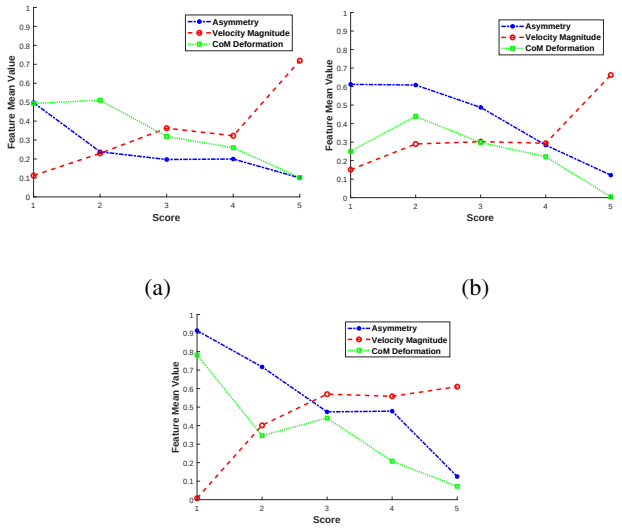

Fig. 10: Features' mean values for the different scores for (a) walking, (b) sitting down, (c) standing up actions

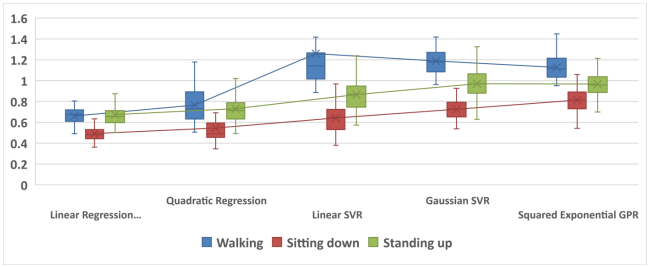

Fig. 11: RMSE for each regression method

this experiment 50 times and reported the Root Mean Square Error (RMSE). Fig. 11 represents the boxplots of the RMSE of the tested models. We can observe that the multiple linear regression model with interactions is the best-fitting model for our data.

Table IV illustrates the mean, maximum, minimum, and median RMSE values of the predicted scores for each action using the multiple linear regression model. The mean plus the standard deviation of the RMSE ranges from 0.56 to 0.79 for all actions, which means that the predicted scores for the majority of the samples are less than one point away from the ground truth scores.

	Walking	Sitting	Standing
Mean $\pm Std$	0.66 ± 0.07	0.49 ± 0.07	0.67 ± 0.12
Max / Min	0.81 / 0.49	0.75 / 0.36	1.03 / 0.50
Median	0.67	0.48	0.66

TABLE IV: Multiple Linear Regression RMSE Statistics

IV. Discussion

A. Discrimination Power of The Features

Each of our proposed features can detect a different trait of motion abnormalities, and no single feature can detect all the types of abnormalities. However, combining these features gives the discrimination power of our feature descriptor. Moreover, in our analysis, we did not find an action-specific trait that is responsible for detecting the abnormality in the performing of a specific action. Therefore, the discrimination power of each feature depends on the apparent trait of the motion abnormality presented in the testing samples. Hence, in this subsection, we are interested in presenting the common apparent trait(s) in the samples of each action included in the two datasets.

Tables V and VI illustrate the capability of each feature to detect motion abnormality if used alone or combined with other features represented by the AUC of the ROC curve and the rank. The rank represents how many actions/datasets where the feature/combination of features was the best among other features/combination of features in discriminating between normal and abnormal action performance. In each row, the best feature/combination of features has been highlighted in bold. For single features, we can observe from Tables V and VI that the most discriminating feature for the walking action is the velocity magnitude feature in both datasets; hence, the slowness of motion is a common trait that appears in the walking action in the two datasets. On the other hand, the CoM trajectory deformation feature is the most discriminating feature for the sitting down action while the asymmetry and the velocity magnitude are interchangeably the second and the third discriminating features. For the standing up action, the discriminating feature differs depending on the dataset; the CoM trajectory deformation feature is the most discriminating trait for the abnormalities presented in the SPHERE dataset, while the asymmetry feature is the most discriminating for samples presented in the EJMQA dataset. For the gait on stairs, we can observe that the CoM trajectory deformation feature is the most discriminating feature for detecting abnormal gait on the stairs followed by the velocity magnitude feature, while the asymmetry feature was not discriminating at all. This is due to the abnormalities being feigned in this action being limited to the left/right leg lead (i.e., left/right leg always steps first) and due to freezing, where the body motion is almost symmetric in all the abnormal sequences. For the rank over all actions, the CoM trajectory deformation feature is ranked high in the SPHERE dataset as it was able to best discriminate normal and abnormal action performance for the sitting down, standing up, and stairs actions. While in the EJMQA dataset, all features received the same rank as each feature was the best for only one action.

For the combination of features, we can observe from Tables V and VI that the optimal performance of our descriptor is achieved by combining all the proposed features as this combination achieved the best rank on both datasets. From the results, we can conclude that the best performance of our proposed method is achieved by using the combination of the three proposed features, and excluding any feature will reduce the performance of our method.

B. Replacing the BOS feature

In this paper, we enhanced our proposed descriptor by replacing the base of support (BOS) feature introduced in our previous work [23] with a better feature, the CoM vertical displacement trajectory feature. In this subsection, we state the reasons for implementing this modification.

It is worth noting that in our preliminary experiments, the BOS feature, approximated as the distance between the knees, was automatically selected as the most discriminating feature between normal and abnormal gait by a feature selection algorithm applied on all pairwise joint distances for the walking action of the SPHERE dataset. However, it carries no diagnosis information for other actions, i.e., sitting down or standing up and in actuality, its value was not able to discriminate between normal and abnormal action performance for these actions. While the BOS feature was not able to discriminate for sitting down and standing up actions, it did not affect the accuracy of classifying action performance into normal and abnormal for the SPHERE dataset as the velocity followed by the asymmetry features were the most discriminating owing to the fact that they were able to split the normal and abnormal samples in the feature space.

Therefore, by replacing this feature with the CoM vertical displacement trajectory defamation feature, we have a more general feature, which can help in abnormality diagnosis for different actions, including gait.

C. Models Comparison

Tables II and III illustrate that the performance of the two models is approximately the same with the GMM's performance being a little better. However, the advantage of using KDE is its non-parametric nature, i.e., it does not have a learning phase. This led to KDE performing faster than DPMM in terms of selecting the appropriate number of clusters followed by the GMM.

D. Comparison to State of The Art

In this section, we compare our results of motion abnormality detection on the SPHERE dataset to the work of Tao et al. [22], as it is the most relevant to our work with the following notes. First, the method of [22] proposed four different models with different tuning parameters. Hence, we compared our results only with the best performing model for each action out of the four models evaluated in [22]. Second, the results listed for the stairs action by [22] are per abnormal event, while ours are per sequence. In doing so, we assume a sequence to be abnormal if it has at least

Feature	Walking	Sitting	Standing	Stairs	Rank
Asymmetry	0.882	0.875	0.826	0.507	0
Velocity Magnitude	**0.988**	0.919	0.993	0.873	1
CoM Trajectory Deformation	0.953	**0.992**	**0.995**	**0.977**	3
Asym. + Vel.	**1**	0.969	**1**	0.701	2
Asym. + CoM	**1**	**1**	0.997	**0.977**	3
Vel. + CoM	0.965	0.992	0.995	**0.977**	1
All together	**1**	**1**	**1**	**0.977**	**4**

TABLE V: Features Discrimination Power Tested on SPHERE Dataset [22] Using KDE (AUC)

Feature	Walking		Sitting		Standing		Rank
	High	Med-Low	High	Med-Low	High	Med-Low	
Asymmetry	0.963 ± 0.03	0.757 ± 0.07	0.960 ± 0.02	0.923 ± 0.04	$\mathbf{0.972 \pm 0.01}$	$\mathbf{0.892 \pm 0.03}$	2
Velocity Magnitude	$\mathbf{1 \pm 0}$	$\mathbf{0.962 \pm 0.027}$	0.885 ± 0.04	0.888 ± 0.02	0.874 ± 0.03	0.535 ± 0.07	2
CoM Trajectory Deformation	0.944 ± 0.03	0.809 ± 0.04	$\mathbf{1 \pm 0}$	$\mathbf{0.990 \pm 0.01}$	0.918 ± 0.02	0.782 ± 0.01	2
Asym. + Vel.	$\mathbf{1 \pm 0}$	0.947 ± 0.06	$\mathbf{1 \pm 0}$	0.970 ± 0.01	0.995 ± 0.01	0.90 ± 0.02	2
Asym. + CoM	$\mathbf{1 \pm 0}$	0.869 ± 0.02	$\mathbf{1 \pm 0}$	$\mathbf{0.996 \pm 0.01}$	$\mathbf{1 \pm 0}$	0.921 ± 0.04	4
Vel. + CoM	$\mathbf{1 \pm 0}$	$\mathbf{0.984 \pm 0.01}$	$\mathbf{1 \pm 0}$	0.993 ± 0.010	0.930 ± 0.03	0.848 ± 0.03	3
All Together	$\mathbf{1 \pm 0}$	0.973 ± 0.03	$\mathbf{1 \pm 0}$	$\mathbf{0.996 \pm 0.01}$	$\mathbf{1 \pm 0}$	$\mathbf{0.923 \pm 0.05}$	**5**

TABLE VI: Features Discrimination Power Tested on EJMQA Dataset Using KDE (Mean AUC $\pm$ Std)

Dataset	Proposed Method		Method of Tao et al. [22]	
	AUC	Model	AUC	Model
Walking	1	GMM/KDE	1	λ_c (JP/2D)
Sitting	1	GMM/KDE	1	λ_d (JP/1D)
Standing	1	GMM/KDE	1	λ_c (JP/3D)
Stairs	1/0.98	GMM/KDE	0.83	λ_d (PJD/2D)

TABLE VII: Comparison to the Method of Tao et al. [22]

Age Range	Normal	High Abnormal	Med-Low Abnormal
$[18-29]$	9.18	4.99	6.28
$[30-39]$	10	3.41	6.12
$[40-49]$	9	4.96	5.18
$[50-59]$	8.19	-	6.17
$[60-69]$	7.47	3.89	6.31
$[70-79]$	-	3.08	5.72
$[80-89]$	-	-	4.87

TABLE VIII: Normalized Walking Action Performance Speed

one abnormal event. For the rest of the actions, the listed results by [22] are per sequence; hence, the results are directly comparable. Table VII illustrates the results of our proposed method for motion abnormality detection compared to the results of [22]. For our results, we used the same three features with all actions while for the results proposed by Tao et al. [22], Table VII illustrates the model, features, and manifold dimensions that produced the best results. Although the results listed in Table VII are of similar values (except in the stairs action), our proposed method uses the same features, modeling approach, and parameters for all actions, which makes it more general. Additionally, our method outperforms the method of [22] in computational overhead, where our method takes approximately 30 seconds to train and less than 1 second to test a sequence, while the method of [22] takes around 2 hours to build the manifold and around 84 seconds to test a sequence on the same machine using published code by the authors.

E. Impact of Aging on the Slowness of Motion

Motion disorders, as well as aging, are the main causes of the slowness of motion. Therefore, in this subsection, we compare the effect of these two causes by measuring the velocity of an action performed by healthy people and patients of different age levels. This is to investigate the probability of the velocity magnitude feature of falsely classifying normal to abnormal due to aging. First, we divided each dataset into age levels, and then we computed the average velocity magnitude feature for each level to measure the average speed of performing the action with/without the existence of an abnormality.

Table VIII illustrates the normalized [5] average velocity magnitude feature of normal and abnormal people at different age levels performing the walking action. We can observe that generally, the average velocity magnitude feature decreases as the age level increases while the abnormality level increases. However, the effect of ageing is lower than the existence of abnormality. This entails that our proposed methods can still function with high accuracy even with increasing age levels.

V. Conclusion and Future Work

The clinical assessment of gait and motion and the interpretation of their abnormalities are crucial for the proper diagnosis and management of neuromusculoskeletal disorders. The ability to detect the presence of motion abnormalities and assess the quality of motion is an add-on in the clinical practice. Due to the aforementioned factors, in this paper, we study, compare, and evaluate two methods of motion abnormality detection and quality assessment. The methods depend on constructing a general descriptor comprising the concatenating of three efficient to compute features and then building a probabilistic/statistical model for motion abnormality detection or a regression model for quantitative motion quality assessment. We tested the proposed methods on different datasets. The results indicate that the proposed methods can detect the abnormality in performing different activities for patients with

[5] We report the normalized average velocity magnitude values on the scale $[0-10]$ so that they are easily comparable; 0 represents no motion, and 10 represents the maximum velocity magnitude that was reached in the dataset.

different types of neuromusculoskeletal disorders and assess the quality of the action performance as well. The proposed methods can be used for in-home monitoring and rehabilitation as well as to assist specialists in performing motion analysis. This work can be extended by considering the limitations of the skeleton data, e.g., limited range (i.e., around 0.5–4 m for MS Kinect V2) and noisy skeletal data in case of occlusion, for more realistic applications where these limitations can prove to be hindrances. One of our extensions in this regard is to use raw depth data to compute the same descriptor in a more robust manner. Furthermore, it would be interesting to evaluate the extent to which the extracted features can be used to classify the type of motion abnormality, e.g., neurological disorders, articular disorders, or orthopedic disorders.

ACKNOWLEDGEMENT

Research partially funded by the Ministry of Higher Education of Egypt, and by EPSRC SPHERE (EP/K031910/1) and University of Bristol International Strategic Fund (ISF).

REFERENCES

[1] D. de Vaus, L. Qu *et al.*, "Demographics of living alone," *Journal of the Home Economics Institute of Australia*, vol. 22, no. 1, p. 27, 2015.

[2] W.-J. J. Yeung and A. K.-L. Cheung, "Living alone: One-person households in asia," *Demographic research*, vol. 32, pp. 1099–1112, 2015.

[3] *People living alone by age and gender 2017 UK Statistic*, (accessed July 2, 2018). [Online]. Available: https://www.statista.com/statistics/281616/people-living-alone-in-the-united-kingdom-uk-by-age-and-gender/

[4] R. M. Kreider and J. Vespa, "The historic rise of living alone and fall of boarders in the united states: 1850–2010," in *Presented at the Population Association of America annual meetings*, 2015.

[5] S. Patel, H. Park, P. Bonato, L. Chan, and M. Rodgers, "A review of wearable sensors and systems with application in rehabilitation," *Journal of neuroengineering and rehabilitation*, vol. 9, no. 1, p. 21, 2012.

[6] A. Ejupi, M. Brodie, S. R. Lord, J. Annegarn, S. J. Redmond, and K. Delbaere, "Wavelet-based sit-to-stand detection and assessment of fall risk in older people using a wearable pendant device," *IEEE Transactions on Biomedical Engineering*, 2016.

[7] P. Pierleoni, A. Belli, L. Palma, M. Pellegrini, L. Pernini, and S. Valenti, "A high reliability wearable device for elderly fall detection," *IEEE Sensors Journal*, vol. 15, no. 8, pp. 4544–4553, 2015.

[8] L. Tong, Q. Song, Y. Ge, and M. Liu, "Hmm-based human fall detection and prediction method using tri-axial accelerometer," *IEEE Sensors Journal*, vol. 13, no. 5, pp. 1849–1856, 2013.

[9] A. T. Barth, B. Boudaoud, J. S. Brantley, S. Chen, C. L. Cunningham, T. Kim, H. C. Powell Jr, S. A. Ridenour, J. Lach, and B. C. Bennett, "Longitudinal high-fidelity gait analysis with wireless inertial body sensors," in *Wireless Health 2010*. ACM, 2010, pp. 192–193.

[10] M. Ye, Q. Zhang, L. Wang, J. Zhu, R. Yang, and J. Gall, "A survey on human motion analysis from depth data," in *Time-of-flight and depth imaging. sensors, algorithms, and applications*. Springer, 2013, pp. 149–187.

[11] E. E. Stone and M. Skubic, "Fall detection in homes of older adults using the microsoft kinect," *IEEE journal of biomedical and health informatics*, vol. 19, no. 1, pp. 290–301, 2015.

[12] G. S. Parra-Dominguez, B. Taati, and A. Mihailidis, "3d human motion analysis to detect abnormal events on stairs," in *2012 Second International Conference on 3D Imaging, Modeling, Processing, Visualization & Transmission*. IEEE, 2012, pp. 97–103.

[13] M. J. Rantz, M. Skubic, C. Abbott, C. Galambos, Y. Pak, D. K. Ho, E. E. Stone, L. Rui, J. Back, S. J. Miller *et al.*, "In-home fall risk assessment and detection sensor system," *Journal of gerontological nursing*, vol. 39, no. 7, pp. 18–22, 2013.

[14] G. Mastorakis and D. Makris, "Fall detection system using kinects infrared sensor," *Journal of Real-Time Image Processing*, vol. 9, no. 4, pp. 635–646, 2014.

[15] S. Gasparrini, E. Cippitelli, S. Spinsante, and E. Gambi, "A depth-based fall detection system using a kinect® sensor," *Sensors*, vol. 14, no. 2, pp. 2756–2775, 2014.

[16] E. E. Stone, M. Skubic, and J. Back, "Automated health alerts from kinect-based in-home gait measurements," in *Engineering in Medicine and Biology Society (EMBC), 2014 36th Annual International Conference of the IEEE*. IEEE, 2014, pp. 2961–2964.

[17] A. P. Rocha, H. Choupina, J. M. Fernandes, M. J. Rosas, R. Vaz, and J. P. S. Cunha, "Kinect v2 based system for parkinson's disease assessment," in *Engineering in Medicine and Biology Society (EMBC), 2015 37th Annual International Conference of the IEEE*. IEEE, 2015, pp. 1279–1282.

[18] O. Ťupa, A. Procházka, O. Vyšata, M. Schätz, J. Mareš, M. Vališ, and V. Mařík, "Motion tracking and gait feature estimation for recognising parkinsons disease using ms kinect," *Biomedical engineering online*, vol. 14, no. 1, p. 97, 2015.

[19] A. Som, R. Anirudh, Q. Wang, and P. Turaga, "Riemannian geometric approaches for measuring movement quality," in *Proceedings of the IEEE Conference on Computer Vision and Pattern Recognition Workshops*, 2016, pp. 43–50.

[20] R. Wang, G. Medioni, C. Winstein, and C. Blanco, "Home monitoring musculo-skeletal disorders with a single 3d sensor," in *Proceedings of the IEEE Conference on Computer Vision and Pattern Recognition Workshops*, 2013, pp. 521–528.

[21] C.-J. Su, "Personal rehabilitation exercise assistant with kinect and dynamic time warping," *International Journal of Information and Education Technology*, vol. 3, no. 4, p. 448, 2013.

[22] L. Tao, A. Paiement, D. Damen, M. Mirmehdi, S. Hannuna, M. Camplani, T. Burghardt, and I. Craddock, "A comparative study of pose representation and dynamics modelling for online motion quality assessment," *Computer Vision and Image Understanding*, vol. 148, pp. 136–152, 2016.

[23] A. Elkholy, M. E. Hussein, W. Gomaa, D. Damen, and E. Saba, "A general descriptor for detecting abnormal action performance from skeletal data," in *Engineering in Medicine and Biology Society (EMBC), 2017 39th Annual International Conference of the IEEE*. IEEE, 2017, pp. 1401–1404.

[24] J. W. Davis and A. F. Bobick, "The representation and recognition of human movement using temporal templates," in *Computer Vision and Pattern Recognition, 1997. Proceedings., 1997 IEEE Computer Society Conference on*. IEEE, 1997, pp. 928–934.

[25] M. A. R. Ahad, J. K. Tan, H. Kim, and S. Ishikawa, "Motion history image: its variants and applications," *Machine Vision and Applications*, vol. 23, no. 2, pp. 255–281, 2012.

[26] M. Plotnik, N. Giladi, Y. Balash, C. Peretz, and J. M. Hausdorff, "Is freezing of gait in parkinson's disease related to asymmetric motor function?" *Annals of Neurology: Official Journal of the American Neurological Association and the Child Neurology Society*, vol. 57, no. 5, pp. 656–663, 2005.

[27] J. C. Wall and G. I. Turnbull, "Gait asymmetries in residual hemiplegia," *Archives of physical medicine and rehabilitation*, vol. 67, no. 8, pp. 550–553, 1986.

[28] J. Jankovic, "Parkinsons disease: clinical features and diagnosis," *Journal of Neurology, Neurosurgery & Psychiatry*, vol. 79, no. 4, pp. 368–376, 2008.

[29] W. F. Abdo, B. P. Van De Warrenburg, D. J. Burn, N. P. Quinn, and B. R. Bloem, "The clinical approach to movement disorders," *Nature Reviews Neurology*, vol. 6, no. 1, p. 29, 2010.

[30] E. M. Gutierrez-Farewik, . Bartonek, and H. Saraste, "Comparison and evaluation of two common methods to measure center of mass displacement in three dimensions during gait," *Human movement science*, vol. 25, no. 2, pp. 238–256, 2006.

[31] A. A. do Carmo, A. F. R. Kleiner, and R. M. Barros, "Alteration in the center of mass trajectory of patients after stroke," *Topics in stroke rehabilitation*, vol. 22, no. 5, pp. 349–356, 2015.

[32] R. Drillis, "Body segment parameters. a survey of measurment technique," *Artit. limbs*, vol. 8, p. 329, 1964.

[33] P. Huber and E. Ronchetti, "Robust statistics–wiley, new york," 1981.

[34] A. P. Dempster, N. M. Laird, and D. B. Rubin, "Maximum likelihood from incomplete data via the em algorithm," *Journal of the royal statistical society. Series B (methodological)*, pp. 1–38, 1977.

[35] C. E. Antoniak, "Mixtures of dirichlet processes with applications to bayesian nonparametric problems," *The annals of statistics*, pp. 1152–1174, 1974.

[36] B. W. Silverman, *Density estimation for statistics and data analysis*. CRC press, 1986, vol. 26.

[37] P. McCullagh, "Regression models for ordinal data," *Journal of the royal statistical society. Series B (Methodological)*, pp. 109–142, 1980.